Available online at www.sciencedirect.com
SCIENCE DIRECT®
Pergamon
Cement and Concrete Research 34 (2004) 1683–1696
CEMENT AND CONCRETE RESEARCH

Formation of ASR gel and the roles of C-S-H and portlandite

Xiaoqiang Hou[a,b,c,*], Leslie J. Struble[b,c], R. James Kirkpatrick[a,c]

[a]Department of Geology, University of Illinois at Urbana-Champaign, Urbana, IL 61801, USA
[b]Department of Civil and Environmental Engineering, University of Illinois at Urbana-Champaign, Urbana, IL 61801, USA
[c]Center for Advanced Cement-Based Materials, University of Illinois at Urbana-Champaign, Urbana, IL 61801, USA

Received 23 September 2003; accepted 18 March 2004

Abstract

Experimental investigations of the reactions between silica, alkali hydroxide solution, and calcium hydroxide show that alkali–silicate–hydrate gel (A-S-H) comparable to that formed by the alkali–silica reaction (ASR) in concrete does not form when portlandite or the Ca-rich, Si-poor C-S-H of ordinary portland cement (OPC) paste is available to react with the silica. Under these conditions, we observe either the formation of additional C-S-H by reaction of $Ca(OH)_2$ with the dissolving silica or the progressive polymerization of C-S-H. The A-S-H dominated by Q^3 polymerization forms only after portlandite has been consumed and the C-S-H polymerized. These conclusions are consistent with previously published results and indicate that the ASR gel of concrete forms only in chemical environments in which the pore solution is much lower in Ca and higher in Si than bulk pore solution of OPC paste. These results highlight the similarity between ASR and the pozzolanic reaction and are supported by data for mortar bar specimens.

Keywords: Alkali–aggregate reaction; ASR gel structure and formation; ^{29}Si NMR Spectroscopy; X-ray diffraction; Calcium–silicate–hydrate (C-S-H)

1. Introduction

The alkali–silica reaction (ASR) in concrete occurs by reaction of certain silica phases in the aggregate with alkali and hydroxide ions in the pore solution of the hydrating cement to produce a hydrous alkali silicate gel [1,2]. This gel can swell by incorporating large amounts of water, causing severe and irreversible expansion and cracking of the concrete. Thus, ASR is an engineering-scale, mechanical process with a chemical origin. Despite decades of study, the chemistry of ASR remains poorly understood.

The ASR gel composition in field concretes varies widely, and it is not clear whether gels with low and high Ca contents should be treated as distinct phases [3]. Compositions typically fall into the range 0.05–0.6 for $(Na_2O+K_2O)/SiO_2$ and 0–0.2 for $(CaO+MgO)/SiO_2$ (molar ratios) [4,5], and they vary significantly with age and distance from the reaction site [3,5,6], especially the Ca content. Knudsen and Thaulow [5] reported that most gels in their study have Na_2O/SiO_2 ratios of 0.2–0.5 and CaO contents from 0% to 20%. Thomas [6] reported that gels in aggregate in a 7-year-old concrete have constant Ca/Si ratios of ~ 0.25 and K/Si ratios of 0.1–0.3, whereas gels in the paste of the same concrete have higher Ca/Si ratios, up to 1.3, and lower K/Si ratios. Many of the gels identified petrographically as ASR gel in that study have compositions very similar to C-S-H.

Helmuth and Stark [7] reviewed ASR gel compositions in detail and concluded that they can be regarded as two-component mixtures containing variable proportions of alkali–calcium–silicate and alkali–silicate components with nearly fixed compositions. The alkali silicate end member is thought to have a composition of 17wt.% (Na_2O+K_2O) and 83% SiO_2, and the alkali calcium silicate end member a composition of approximately 6.6% (Na_2O+K_2O), 52.6% CaO, and 40% SiO_2. This idea is consistent with the earlier model of Powers and Steinour [8,9], which Stark [10] considers to best fit most of the published observations on ASR. In contrast, in a study of ASR in mortars made with high alkali cement and opal-bearing natural sand, Diamond [3] concluded that ASR gel is neither consistently low nor high in Ca, but varies from one grain to another. He reported that the compositions of individual grains span almost the full range of known gel compositions and concluded that ASR gel has a complex and highly

* Corresponding author. Department of Geology, University of Illinois at Urbana-Champaign, Urbana, IL 61801, USA. Tel.: +1-217-244-2355; fax: +1-217-244-4996.
E-mail address: xhou@uiuc.edu (X. Hou).

0008-8846/$ – see front matter © 2004 Elsevier Ltd. All rights reserved.
doi:10.1016/j.cemconres.2004.03.026

variable chemical composition and that the compositional model of Helmuth and Stark [7] may be useful but not universal. It is important to note that most published analyses of ASR gel were obtained by energy-dispersive X-ray (EDX) spectroscopy methods using a scanning electron microscope, and because the excitation volumes analyzed are of the order of several cubic microns, they may contain phases other than ASR gel.

The presence of calcium appears to be essential for concrete expansion due to ASR, but its role is controversial. Calcium-rich, C-S-H-type gels in cement paste have little swelling capacity, but many workers [6,11–14] have concluded that calcium is necessary for the formation of ASR gel. Thomas [14] showed that significant expansion occurs only when sufficient reactive CH is available, that systems without CH exhibit little expansion despite evidence that ASR has occurred, and that in the absence of CH, silica remains in solution and reaches concentrations as high as 0.5 M SiO_2. This result verified earlier indications [11,12,15] that ASR gel does not form in the absence of Ca^{2+}. Wang and Gillott [16] concluded that CH both acts as a buffer to maintain a high OH^- concentration in the pore solution and exchanges for alkali in the ASR gel, leading to alkali release and further production of swelling alkali silicate gel. Thomas [6] similarly presented compositions of gels near or within aggregate grains and far from aggregate grains as evidence for replacement and recycling of alkalis. Gaboriaud et al. [17] suggested that Ca^{2+} may play a catalytic role by promoting cross-linking of silicate ions in solution during the gelation process. Monteiro and colleagues [18–20] used electric double-layer theory to explain the effect of Ca on the behavior of ASR gels. They proposed that relatively large expansive pressures are expected to develop when the negative charges of the silica particles are offset by a diffuse layer containing monovalent ions such as Na^+ and K^+, whereas smaller pressures develop when the diffuse layer contains ions of higher valence such as Ca^{2+}. The role of Ca in ASR remains controversial and is one focus of the investigation presented here.

Published XRD and scanning electron microscopy (SEM) observations suggest that ASR gel has a poorly ordered layered structure [3,21,22], and early ^{29}Si magic angle spinning (MAS) NMR spectroscopy [23] showed that identified ASR gels are dominated by Q^3 silicate polymerization, consistent with dominantly a layer silicate structure. In the presence of calcium, the spectra also contain Q^1 and Q^2 peaks for Si sites in C-S-H. Subsequent studies by Brough et al. [24] confirmed these conclusions and demonstrated that the C-S-H coexisting with ASR gel is more polymerized than the C-S-H formed during hydration of ordinary portland cement (OPC). These results are consistent with more recent studies that demonstrate the coexistence of an alkali-rich silicate gel low in calcium and a more calcium-rich, C-S-H-like phase that contains some alkali [6,14,24–27]. The C-S-H phase is thought to have limited swelling capacity [3,28]. Wieker et al. [29–31] also concluded that ASR gel structure is dominated by silicate tetrahedra with Q^3 polymerization and, controversially, proposed that the structure is similar to that of kanemite ($NaHSi_2O_5{\cdot}3H_2O$), a layer-structure hydrous Na silicate [32–34]. Our recent NMR, XRD, and compositional studies of natural and synthetic ASR gels [26,27] have confirmed the presence of kanemite-like structural units in ASR gel, although the actual structure is probably more complex. Our results [26,27] also show that the local structures of the synthetic and field gels are quite similar, with basal XRD peaks near 0.8–1.2 nm and ^{29}Si NMR spectra dominated by peaks for Si sites with layer structure Q^3 polymerization, although Q^4, Q^2, and Q^1 sites are also present. The compositional and ^{29}Si NMR data indicate that there is insufficient alkali to charge-balance all the nonbridging oxygens and, thus, that there is a significant concentration of Si–OH linkages, as is the case for kanemite. We call this phase alkali–silicate–hydrate (A-S-H). Other researchers have identified zeolitic phases in ASR products [35–37], but those samples may have been impure or recrystallized.

In the present research, we conducted model experiments to simulate ASR formation in concrete, with the specific objectives of evaluating changes in A-S-H and C-S-H composition and structure during ASR gel formation; the microstructural relationships between the aggregate, A-S-H, and C-S-H; the effects of aggregate mineralogy; and the effects of K^+ versus Na^+. The reaction products were characterized as a function of time using XRD, ^{29}Si MAS NMR, chemical analysis, optical microscopy, and SEM. The most important result is that A-S-H does not form from reactive aggregate until all available $Ca(OH)_2$ has been consumed to form C-S-H. Thus, as proposed by Taylor [38], the ASR and pozzolanic reactions are closely associated in concrete, except that the pozzolanic reaction proceeds before the formation of A-S-H.

2. Experimental

2.1. Sample preparation

Most of the experiments involved reaction between aggregate powder and NaOH or KOH solution, with and without $Ca(OH)_2$. The procedure was similar to that reported by Cong et al. [23]. Three aggregates were used: opal (Virgin Valley, NV, Ward's Natural Science Establishment), Vycor glass (Corning), and Ottawa sand (US Silica). The A-S-H gel was detected for only the opal and Vycor glass. The aggregates were first ground and sieved to a particle size less than 300 μm (instead of the 30 μm used by Cong et al. [23]) and were then reacted with 1 M NaOH or KOH solution with or without solid $Ca(OH)_2$. In all of the experiments with $Ca(OH)_2$, the aggregates were dry blended with reagent-grade $Ca(OH)_2$ (Fisher Scientific). The large aggregate particle size was chosen to facilitate SEM obser-

vation. Table 1 summarizes the batch compositions. After dry blending, 1 M NaOH or KOH solution was added to the powder and mixed with magnetic stirring to obtain a homogeneous slurry under N_2 flow to avoid carbonation. The slurry was then subdivided and placed in individual 30-ml polyethylene bottles and stored at room temperature. Reactions were stopped at 1, 7, 21, 65, 150, 264, and 360 days by removing the fluid through a 45-μm filter and washing the solid with acetone. Solid products were dried at room temperature in a vacuum oven and examined by XRD, ^{29}Si MAS NMR, optical microscopy, and SEM-EDX.

Experiments were also conducted with larger cubes of the Nevada opal and Vycor glass immersed in NaOH solution with or without $Ca(OH)_2$. In many ways, these experiments were similar to those of Dent Glasser and Kataoka [2] with synthetic silica gel, but our focus is on characterization of the solid reaction products. The aggregate cubes, 0.64 cm on each side, were placed in 30-ml polyethylene bottles. For the preparations containing calcium, $Ca(OH)_2$ powder surrounded the cube up to its top, and 10 ml of solution was added to each bottle. Table 2 lists the amounts of each component used in these experiments. The mixtures were held without stirring in a laboratory oven at 80 °C for 1 day to simulate the conditions of ASTM C 289. After reaction, the aggregate cubes were weighed and examined. In the samples of opal + NaOH + $Ca(OH)_2$, a substantial amount of hard, white precipitate formed on the opal cubes. This precipitate was peeled off after drying at room temperature, and its powder XRD pattern and ^{29}Si MAS NMR spectrum were collected.

Samples of mortars subjected to ASTM C 1260 were examined using XRD and ^{29}Si MAS NMR. These samples were made following the standard procedure [39] and contained either opal (5% opal plus 95% limestone) or Vycor glass (100%) and Type I portland cement (Lone Star Industries) with a total alkali content of 0.8% (by weight, expressed as equivalent Na_2O). After 15 and 28 days of immersion, small pieces were cut from each bar, ground, washed with acetone, and dried in a vacuum oven for examination.

Table 1
Batch compositions for aggregate powder reactions

System	Aggregate (powder) (g)	MOH (1 M) (M = K, Na) (ml)	$Ca(OH)_2$ (powder) (g)	Bulk atomic ratio
Opal + NaOH	112.5	500	0	Na/Si = 0.29,[a] Ca/Si = 0
Opal + NaOH + $Ca(OH)_2$	112.5	500	37.05	Na/Si = 0.29, Ca/Si = 0.29
Vycor + NaOH	112.5	500	0	Na/Si = 0.27, Ca/Si = 0
Vycor + NaOH + $Ca(OH)_2$	112.5	500	37.05	Na/Si = 0.27, Ca/Si = 0.27
Vycor + KOH	112.5	500	0	K/Si = 0.27, Ca/Si = 0
Vycor + KOH + $Ca(OH)_2$	112.5	500	37.05	K/Si = 0.27, Ca/Si = 0.27
Sand + KOH	112.5	500	0	K/Si = 0.27, Ca/Si = 0
Sand + KOH + $Ca(OH)_2$	112.5	500	37.05	K/Si = 0.27, Ca/Si = 0.27

[a] The opal contains 93.2% SiO_2, Vycor glass contains 97% SiO_2, and Ottawa sand contains 100% SiO_2.

Table 2
Batch compositions for aggregate cube reactions

System	Aggregate[a] (g)	NaOH (1 M) (ml)	$Ca(OH)_2$ (powder) (g)	Bulk atomic ratio	Weight loss after 1 day (%)
Opal + NaOH	2.7135	10	0	Na/Si = 0.24, Ca/Si = 0	24.6
Opal + NaOH + $Ca(OH)_2$	2.7100	10	1.0000	Na/Si = 0.24, Ca/Si = 0.32	33.6
Vycor + NaOH	3.0432	10	0	Na/Si = 0.20, Ca/Si = 0	0.1
Vycor + NaOH + $Ca(OH)_2$	3.0419	10	1.0000	Na/Si = 0.20, Ca/Si = 0.27	0.2

[a] Five cubes in each case. The listed mass here is the total for the five cubes.

2.2. Sample examination

The ^{29}Si MAS NMR spectra were recorded at room temperature using a spectrometer (Varian UNITY INOVA 500WB) equipped with an 11.74T superconducting magnet (Oxford Instrument) and a 7-mm MAS probe (Doty Scientific). The spinning frequency was ~ 8 kHz, and $\pi/4$ pulses and 50-s recycle times were used. Longer recycle times were tried but no significant signal gain was observed, except that the intensity of the Q^4 resonance for Vycor glass increased (silica glasses have extremely long T_1 relaxation times), but this increase was not important because we did not attempt quantitative analysis of the Vycor signal intensity. Normally about 200–300 scans were accumulated for each sample. The probe housing produces a broad, ill-defined ^{29}Si chemical shift anisotropy (CSA) powder pattern to the left of the sample resonances, and the rotor produces a sharp MAS resonance at −48.5 ppm with an associated spinning side band that is sometimes visible near −120 ppm. The background does not affect data quality or interpretation.

The XRD patterns were recorded for powders vacuum-dried at room temperature and for pastes made by rehydrating some dried samples to evaluate their expansion behavior. A Rigaku diffractometer was used with CuK_α radiation, a scanning rate of 1° 2θ per min, and a step size of 0.02° 2θ. Kaolinite (KGa-1, Clay Minerals Repository, University of Missouri-Columbia) was used as an external XRD standard.

Optical microscopy and SEM were used to characterize the microstructural development. Microscope specimens were prepared by mixing powders of the dried reaction products with epoxy, and after specimens were hardened,

they were ground and polished into thin sections. For the samples containing $Ca(OH)_2$, the reaction products formed solid blocks after 7 days, and some of these specimens were made without breaking them into powders or washing them in acetone.

Optical microscopy used a Zeiss Axiovert 135 microscope equipped with incident halogen illumination and both transmitted and reflected light optics and a digital image capture system. The SEM-EDX examination was performed using a Philips XL30 ESEM-FEG field-emission environmental scanning electron microscope (ESEM-FEG) with EDX. The working distance was 10 mm, optimized for EDX. The accelerating voltage was 15 kV and the electron beam diameter was normally ~ 20 nm.

Two solution samples obtained after filtration of the solids in samples of opal + NaOH and opal + NaOH + $Ca(OH)_2$ were analyzed for Si, Na, and Ca concentrations using inductively coupled plasma emission spectroscopy (ICP-AES) at the University of Illinois Micro-Analytical Laboratory. Both samples were filtered after 21 days of reaction. The concentrations of the two solutions are as follows: [Si] = 1.20 M and [Na] = 0.82 M for opal + NaOH; and [Si] = 0.28 M, [Na] = 0.63 M and [Ca] = 0.01 mM for opal + NaOH + $Ca(OH)_2$.

3. Results and interpretation

3.1. Aggregate reaction mixtures

The data for the reaction mixtures containing aggregate powders and alkali hydroxide solution with and without $Ca(OH)_2$ provide clear evidence for significant reaction and time-dependent changes. The macroscopic appearance of these mixtures varies greatly with time and starting materials. In experiments without $Ca(OH)_2$, the amount of residual solid decreases appreciably with increasing reaction time. The dissolved Si concentration of 1.2 M in the 21-day opal + NaOH sample indicates substantial dissolution of the aggregate under these conditions. In contrast, in the experiments containing $Ca(OH)_2$, the amount of residual solid did not decrease appreciably, and the solids became cemented after 7 days for opal and 21 days for Vycor. The lower level of dissolved Si (0.28 M in the 21-day sample) and residual Na concentration indicates significant silicate precipitation and greater Na incorporation in the reaction products.

3.1.1. Opal + NaOH + $Ca(OH)_2$

Powder XRD patterns of the opal + NaOH + $Ca(OH)_2$ samples show significant and progressive changes with increasing reaction time that indicate loss of opal and formation of C-S-H (Fig. 1a). The starting opal yields characteristic XRD peaks at 22° and 35.8° 2θ with a shoulder at 21° [40]. The sample reacted for 1 day shows only diffraction peaks for opal and portlandite. At 7 days, broad peaks at 1.24 nm (7.15° 2θ) and 0.305 nm (29.2° 2θ) appear. These are readily assigned to tobermorite-type C-S-H [41], and the basal peak at 1.24 nm indicates reasonable crystallinity. At 21 days, these two peaks increase in relative intensity but the basal peak becomes less well defined. In parallel, the portlandite peaks disappear at 21 days, indicating its complete consumption by this time. There are no further substantial changes in the XRD patterns for samples reacted for 150–360 days, and opal remains present at all times. The XRD patterns of rehydrated pastes of the 7- and 150-day samples show no change in the position of the diffraction at 7.15° 2θ, indicating no basal expansion of the C-S-H due to water.

Parallel changes in the ^{29}Si MAS NMR spectra of these samples indicate substantial increase in the silicate polymerization of the C-S-H as reaction proceeds and the formation and subsequent transformation of A-S-H (Fig. 1b). The starting opal yields a large, broad peak at −112 ppm, a smaller peak centered at −103 ppm, and an even smaller peak at −94 ppm. These are characteristic, respectively, of Q^4, Q^3(1OH) and Q^2(2OH) sites of opal and other amorphous hydrous silicas [23,40]. The peak at −122 ppm is a spinning side band associated with probe background. Peaks at −79 and −85 ppm first appear at 1 day, and these are readily assigned to Q^1 and Q^2 Si sites in C-S-H [23,42,43,49]. The relative intensity of the Q^3(1OH) opal peak also decreases at 1 day, and the opal Q^2(2OH) peak is hardly visible. These changes indicate preferential reaction of Si sites with direct Si–OH linkages, consistent with previous reports [1]. At 7 days, the relative intensities of the resonances at −79 and −85 ppm increase greatly at the expense of the signal for opal. In this sample, the opal Q^4 peak represents only about 36% of total Si in the solids, indicating significant reaction progress. The Q^1/Q^2 ratio for the C-S-H in this sample is 1.1, indicating a relatively depolymerized structure, quite similar to the C-S-H formed in equilibrium with $Ca(OH)_2$ in synthesis experiments [42]. At 21 days, C-S-H is represented by peaks at −79, −82, and −85 ppm, and the relative intensity of the −85 ppm peak is now greater than the others, similar to the relatively polymerized C-S-H formed in synthesis experiments in the absence of $Ca(OH)_2$, which XRD shows has disappeared at this time in our experiments. Resolution of the peak at −82 ppm indicates a quite well crystallized phase. The relative intensity of the Q^4 peak for residual opal is 24%, indicating continued reaction. In addition, this sample yields broad peaks at −88 and −95 ppm, which are readily assigned to Q^2 and Q^3 peaks of A-S-H [23,24]. There is also a small peak at −71 ppm, representing a trace amount of Si with Q^0 polymerization, which may be residue from the aqueous phase.

The number and relative intensities of the ^{29}Si NMR resonances do not change significantly with increasing reaction time beyond 21 days, paralleling the XRD results. The proportion of Si in residual opal remains approximately 22% up to 360 days. The resonances for C-S-H and A-S-H broaden and become less well resolved, however, indicating

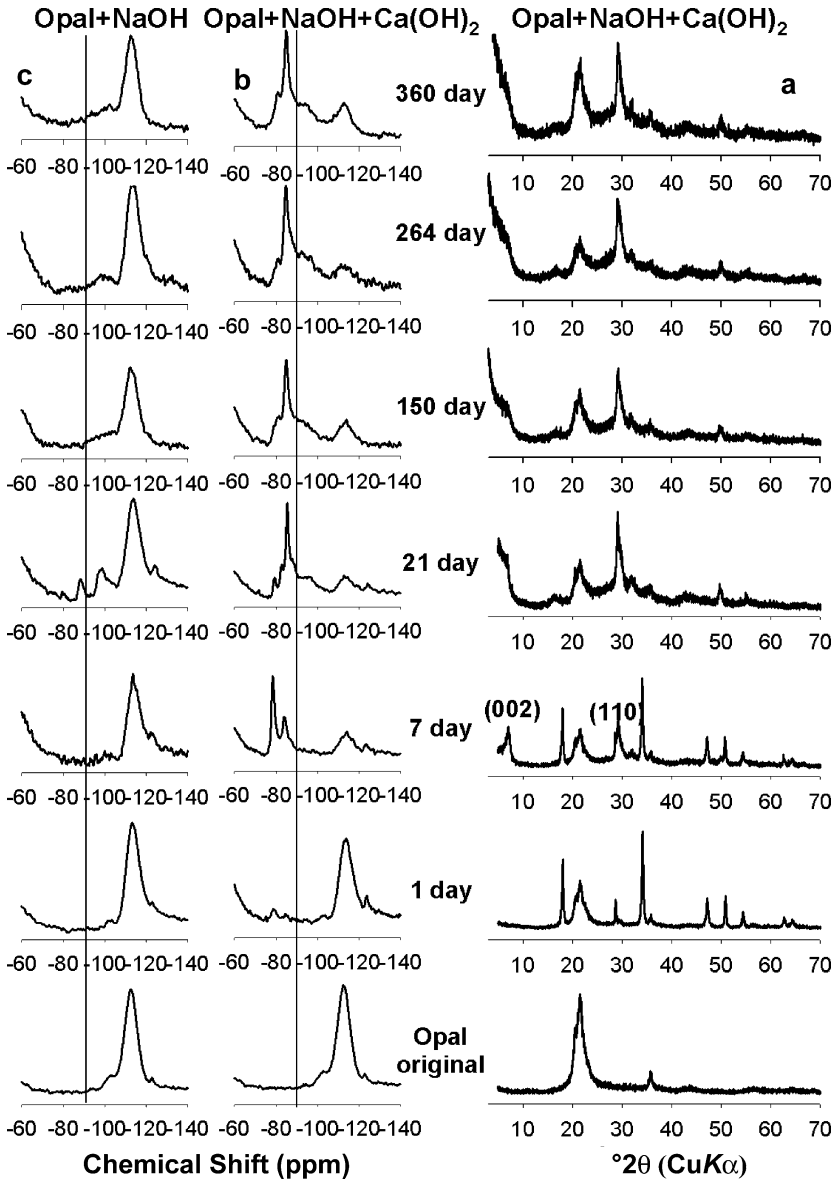

Fig. 1. (a) Powder XRD patterns of starting opal and selected reaction mixtures with $Ca(OH)_2$ and NaOH solution at the indicated reaction times, (b) ^{29}Si MAS NMR spectra of starting opal and selected reaction mixtures with $Ca(OH)_2$ and NaOH solution at the indicated reaction times, and (c) ^{29}Si MAS NMR spectra of reaction mixtures of opal with NaOH solution only at the indicated reaction times.

decreased structural order and paralleling the decreased resolution of the C-S-H basal peak in XRD.

Overall, the results reported above are very similar to those of Cong et al. [23]. Their work did not include short-time experiments, and, thus, they did not observe spectra showing less polymerized C-S-H with Q^1/Q^2 ratios greater than 1, such as those of the 1- and 7-day samples here. The increase in C-S-H polymerization with increasing reaction time is a key to understanding the chemical relationships between C-S-H and A-S-H and is discussed later.

Optical microscopy and SEM-EDX show progressive microstructural changes that parallel the XRD and NMR results. The majority of starting opal grains are angular, uniform, and nearly structureless at low magnifications (Fig. 2a), although a small fraction contains 1- to 2-μm pores, and at very high magnifications there are regions that contain pores in the 50- to 100-nm range (Fig. 2b). After 1 day of reaction, the opal grains show little change except for a slight increase in the optical birefringence of some particles under reflected, cross-polarized light. At 7 days, most opal particles have considerable porosity, and few remain homogeneous. At longer reaction times, the average pore size increases, and some grains are highly porous (Fig. 3a–d). Many of the grains contain rounded to subangular volumes that show only Si and O in EDX analysis and are residual opal. Thus, dissolution of the opal occurs both at the exterior surfaces and internally, consistent with Diamond's observation [3]. SEM-EDX analysis shows the presence of

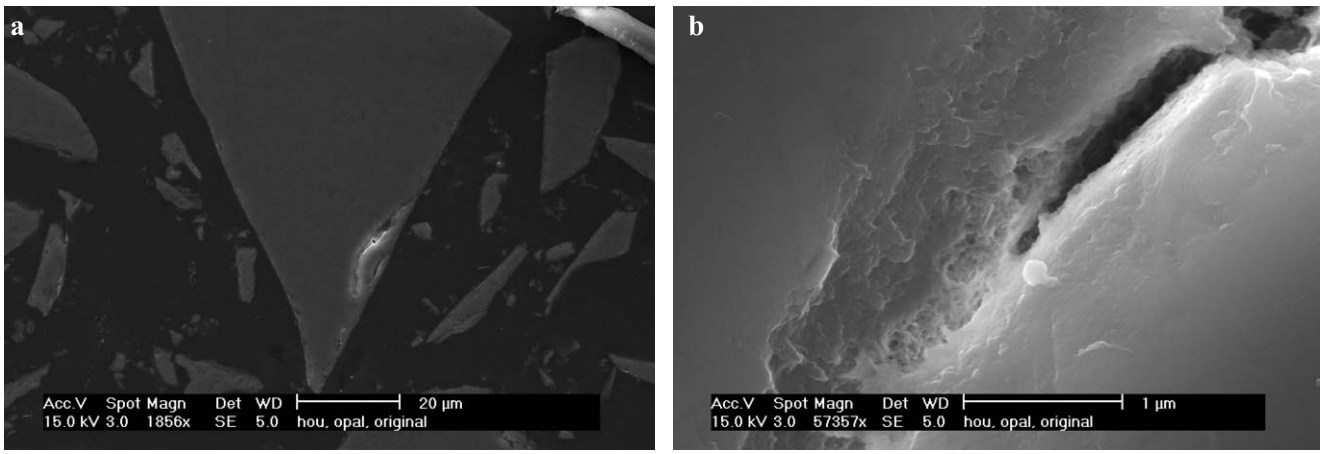

Fig. 2. SEM images of starting opal showing its generally uniform microstructure but with pores on the micrometer and 50- to 100-nm scales as seen in (b), which are probably responsible for the relatively high reaction rate of opal in ASR.

A-S-H with Na and Ca located within many of the original opal grains and surrounding the residual rounded opal volumes (e.g., Fig. 3b). Optical examination shows that the aggregate particles are cemented by C-S-H that is more reflective than the opal in reflected light and less transparent in transmitted light. The C-S-H often shows undulatory extinction or birefringence. SEM-EDX shows that the C-S-H contains much more Ca than the A-S-H and a variable amount of Na. The structural location of this Na is unclear. It may be in the C-S-H, in A-S-H intimately mixed with the

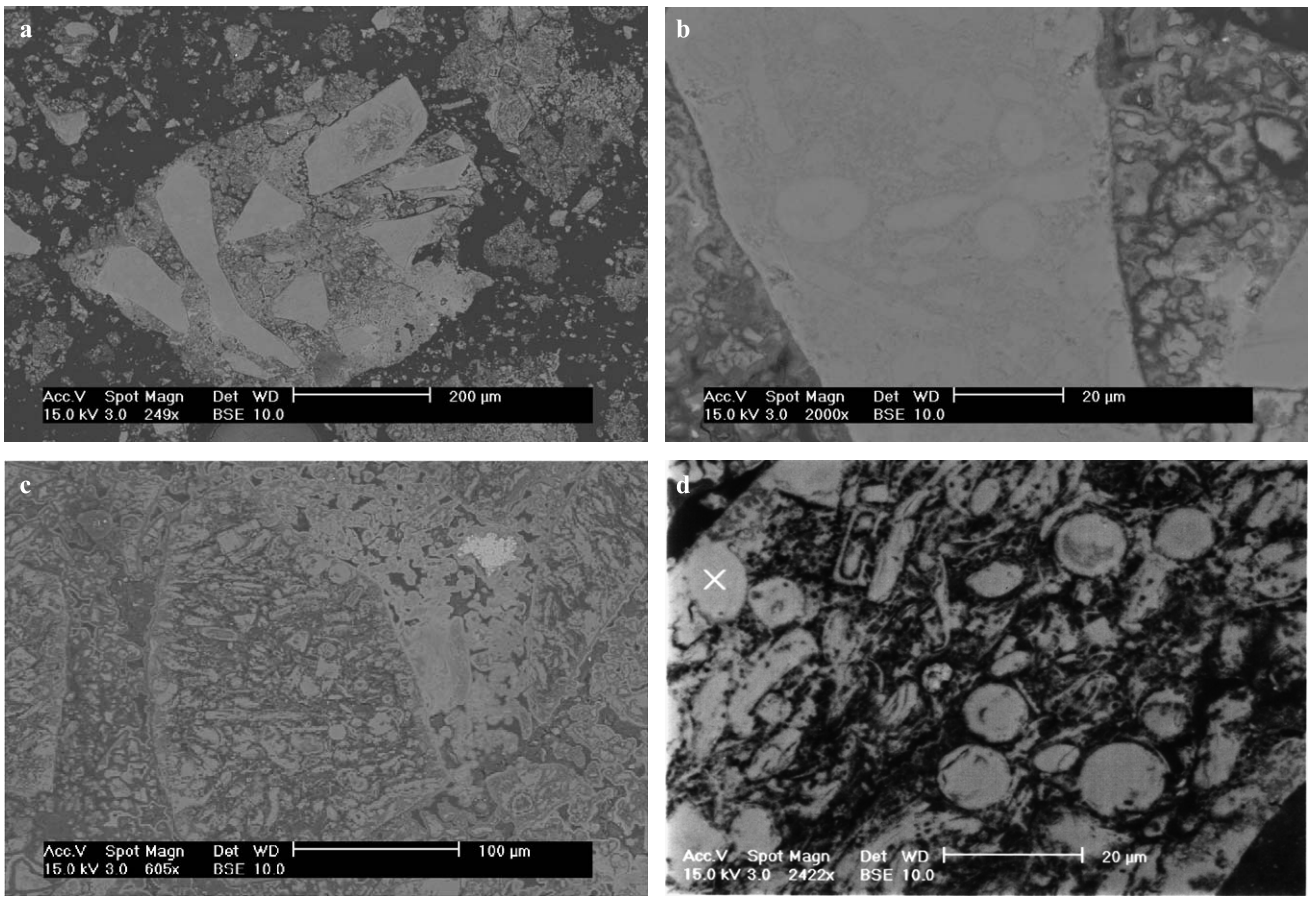

Fig. 3. Backscattered secondary electron (BSE) images of opal reacted with $Ca(OH)_2$ and NaOH solution for 21 days. (a) A typical aggregation of opal grains containing A-S-H and aggregated by C-S-H; (b) details of opal grain containing A-S-H showing less bright A-S-H and brighter, rounded volumes of residual opal; (c) and (d) more extensively dissolved opal grains containing significant porosity.

C-S-H on the scale of a few micrometers, or precipitated from the aqueous solution during the acetone washing.

3.1.2. Opal + NaOH

The XRD patterns for the opal + NaOH solution experiments contain only peaks for opal and show little change with reaction time (data not shown), but the ^{29}Si MAS NMR spectra show new peaks that can be attributed to the formation of A-S-H and its progressive structural reorganization (Fig. 1c). At 1 and 7 days, there are no substantial changes to the NMR spectra, except that the peak representing Q^3(1OH) sites in opal at −103 ppm decreases slightly in intensity. At 21 days, there are three new peaks at −79.5, −88.2, and −98.6 ppm that can be assigned to Q^1, Q^2, and Q^3 sites in an A-S-H, respectively [23,24]. With increasing reaction time, the resonances at −79.5 and −88.2 ppm decrease in intensity, and the resonance at −98.6 ppm broadens and overlaps the Q^3 peak due to residual opal. Similar NMR signatures have been observed previously in model ASR experiments and are attributable to gelation of the solution followed by its progressive structural reorganization [24]. In high-pH solutions such as those in cement paste, silicate is present in a wide range of polyatomic anions with many polymerization states [44–48]. As the

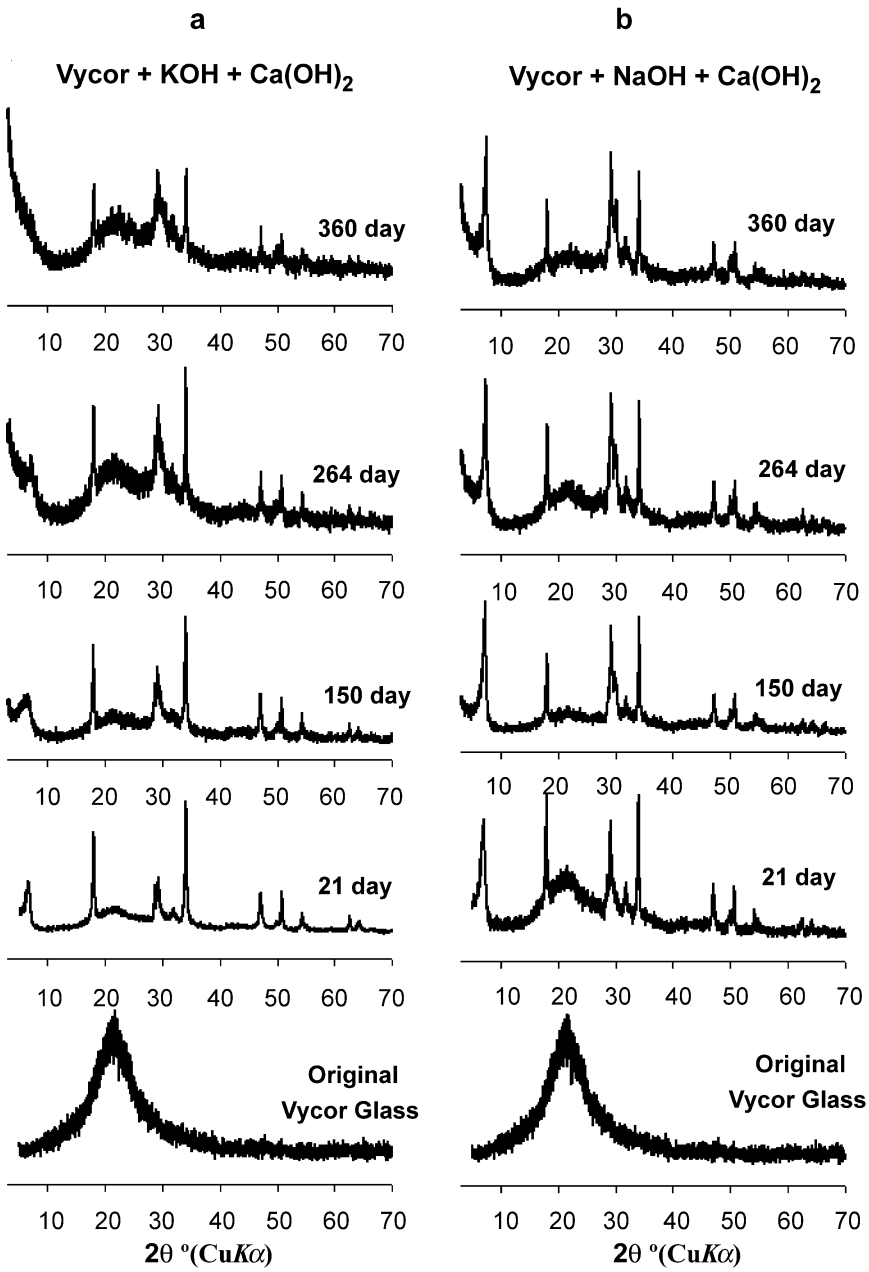

Fig. 4. Powder XRD patterns of Vycor glass reacted with (a) $Ca(OH)_2$ and KOH solution and (b) $Ca(OH)_2$ and NaOH solution for the indicated times.

silicate concentration increases, these polyions begin to cross-link, eventually forming solid gel. Because the silicate consists of cross-linked polyanions, there is relatively little local bond angle disorder, and the ^{29}Si NMR peaks are relatively narrow, as observed here for the 21-day sample. For the A-S-H of our experiments, this initial structure reorganizes with increasing time, becoming progressively more cross-linked, as evidenced by the increased intensity at more negative chemical shifts. The increased peak widths indicate a parallel increase in bond angle disorder. As discussed in our previous papers [26,27], sheetlike structural units dominate A-S-H in the compositional range that occurs in cement pastes. Calculations based on the relative abundances of the sites observed by ^{29}Si NMR and the solution chemical compositions for the 21-day sample here show that the atomic Na/Si ratio of the A-S-H is approximately 0.4, coincidentally identical to that of the A-S-H gel from the in-service concrete we examined [26,27].

Degradation of the opal is slower in the experiments with pure alkali solutions than in those containing Ca. At 21 days, the opal + NaOH + $Ca(OH)_2$ sample has a dissolved Si concentration of 0.28 M, and opal accounts for 24% of the total solid based on ^{29}Si NMR data, indicating dissolution of 78% of the opal at that time. In contrast, only 47% of the opal has dissolved in the 21-day opal + NaOH sample, even though the analyzed dissolved Si concentration is 1.2 M.

Development of porosity within opal grains in the opal + NaOH samples as observed in optical microscopy is similar to that in the samples with Ca, although because no C-S-H is produced the opal grains are not aggregated.

3.1.3. *Vycor + NaOH or KOH + Ca(OH)$_2$*

Experiments with Vycor glass, $Ca(OH)_2$, and either NaOH or KOH show progressive changes similar to those with opal, and the changes observed provide well-defined and important information about the reaction sequence. The reaction rate is much slower than with opal, however, and complete loss of $Ca(OH)_2$ and full conversion to highly polymerized C-S-H does not occur even at 360 days (Figs. 4 and 5). At 1 day, XRD (Fig. 4) shows only a broad diffraction with a maximum at 22° 2θ, characteristic of SiO_2 glass, and narrower peaks for portlandite. At 7 days, there is an additional, very small peak at 7° 2θ (1.26 nm) with NaOH and 6.6° 2θ (1.33 nm) with KOH, indicating the initial appearance of C-S-H. At 21 days and longer, the basal C-S-H peaks are much larger, and C-S-H peaks are present at 29.2° (0.31 nm) and 31.7° (0.27 nm) and increase in intensity with increasing reaction time. The peaks for portlandite and Vycor glass remain even at 360 days, but decrease in intensity with increasing reaction time for both the NaOH and KOH samples. The basal and (*hk*0) peaks for C-S-H are consistently sharper and better resolved for the Vycor experiments than for the corresponding opal experiments, indicating greater structural order, perhaps due to the slower reaction rates. As with opal, XRD patterns of pastes made with the reaction products show no expansion of the C-S-H basal spacing.

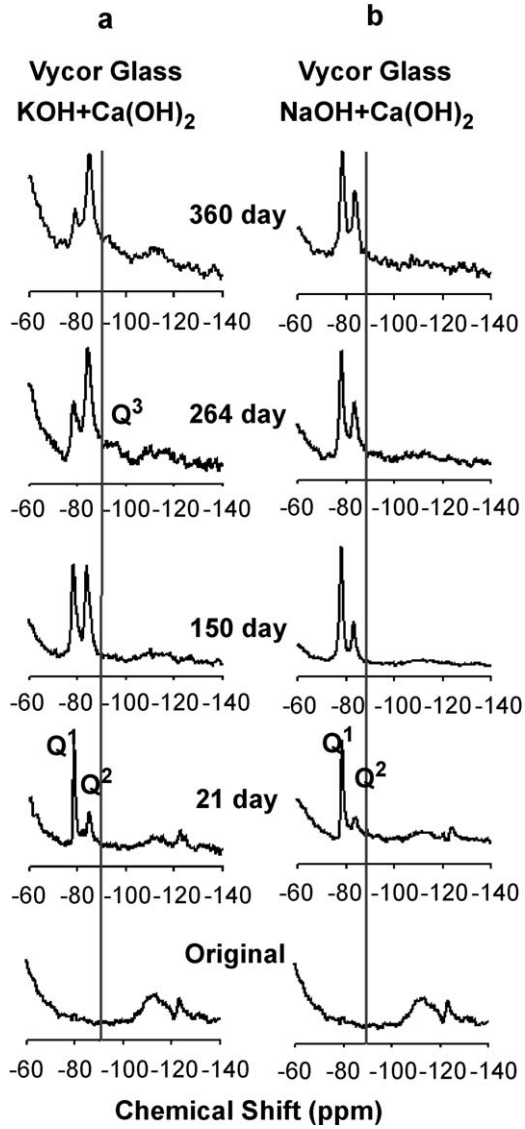

Fig. 5. ^{29}Si MAS NMR spectra of Vycor glass reacted with (a) $Ca(OH)_2$ and KOH solution and (b) $Ca(OH)_2$ and NaOH solution for the indicated times.

The ^{29}Si MAS NMR data (Fig. 5) confirm the formation of C-S-H, show progressive increase in its polymerization, and show formation of A-S-H with increasing reaction time, similar to the results with opal described above. The spectrum of unreacted Vycor glass contains a broad resonance centered at −112 ppm, representing Q^4 structural sites, as expected for silica glass. The ^{29}Si T_1 relaxation time of Vycor appears to be very long, and its spectrum has a poor signal/noise ratio. Quantitative determination of its relative abundance is not possible, although its relative peak area generally decreases with reaction time. At 1 day, the spectra are the same as for the starting Vycor glass. At 7 days, there are weak resonances at −79 and −85 ppm representing a trace of C-S-H, as also

observed by XRD. At 21 days, the two C-S-H resonances have increased intensity, and the Q^1 peak at −79 ppm is clearly dominant for both the NaOH and KOH experiments. With increasing reaction time up to 360 days, the Q^1/Q^2 ratio decreases, and the rate of decrease is greater for KOH than for NaOH. For the KOH system, this ratio decreases from 1.8 at 21 days to 0.9 at 150 days, 0.5 at 264 days, and 0.3 at 360 days. For the NaOH system, it decreases from 4.2 at 21 days to 3.2 at 150 days, 1.8 at 264 days and 1.2 at 360 days. The rate of decrease, and thus the rate of change of C-S-H polymerization, in both sets of experiments with Vycor is significantly slower than observed for opal, for which the Q^1/Q^2 ratio decreases from 1.1 at 7 days to 0.2 at 21 days (the peak at −82.5 ppm is counted as Q^2). This observation may suggest that the overall reaction rate for C-S-H polymerization is limited by the rate of dissolution of silica.

The ^{29}Si NMR spectra of the experiments with KOH also contain weak resonances near −95 ppm after Q^2 becomes dominant in C-S-H at 264 and 360 days, indicating the formation of some A-S-H. These samples show the greatest reduction in $Ca(OH)_2$ by XRD. None of the Vycor samples with NaOH + $Ca(OH)_2$, whose C-S-H is always dominated by Q^1 sites, show evidence of A-S-H formation.

Optical microscopy and SEM-EDX show progressive microstructural changes that parallel the XRD and NMR results. Most of the starting Vycor grains are very uniform and structureless, except that some contain cracks. After 1 day of reaction, the Vycor grains show no change, but some portlandite particles are attached to Vycor surfaces. At 7 days, some of the smaller Vycor grains occur in aggregations bound by a matrix of portlandite and C-S-H, and these aggregations show higher collective birefringence than individual Vycor grains under reflected, cross-polarized light. At 21 days, most of the Vycor grains occur in aggregations bound by C-S-H and portlandite (Fig. 6a, b). In addition, essentially all of the Vycor grains have nearly continuous rims of dense C-S-H on their exterior surfaces; these appear much brighter than Vycor in backscattered SEM images (Fig. 6a, b). In some cases this dense C-S-H also occurs in what appear to be cracks in the original Vycor grains (Fig. 6b). The Vycor grains do not develop internal porosity and normally yield signal for only Si and O in EDX analysis.

3.1.4. *Vycor + NaOH or KOH*

As observed in the opal + NaOH experiments, the XRD patterns of the Vycor + KOH and Vycor + NaOH samples are identical to that of the starting Vycor glass, indicating that no crystalline phases form. Similarly, the ^{29}Si MAS NMR spectra of most of the samples examined, including Vycor + KOH at 360 day and Vycor + NaOH at 21, 150, and 360 days, contain signal for only Vycor. Only the 21-day Vycor + KOH sample shows additional signals, which occur at −79.5, −88.0, and −97.5 ppm (data not shown) and are very similar to those of the A-S-H gel in the 21-day opal + NaOH sample described above.

3.2. *Aggregate cubes*

Experiments with opal and Vycor cubes immersed in NaOH solution or NaOH solution and solid $Ca(OH)_2$ add important insight into the reactions that form A-S-H and confirm that A-S-H is formed only with relatively polymerized C-S-H. After 1 day at 80 °C, the opal cubes in NaOH solution have a weight loss of 24.6% (producing a calculated dissolved silica concentration of about 1.0 M), and the opal cubes in the mixture of NaOH and $Ca(OH)_2$ have a weight loss of 33.6% (Table 2). Vycor shows weight losses of only 0.1% in NaOH and 0.2% in NaOH + $Ca(OH)_2$. Thus the rate of reaction of opal is much faster than that of Vycor,

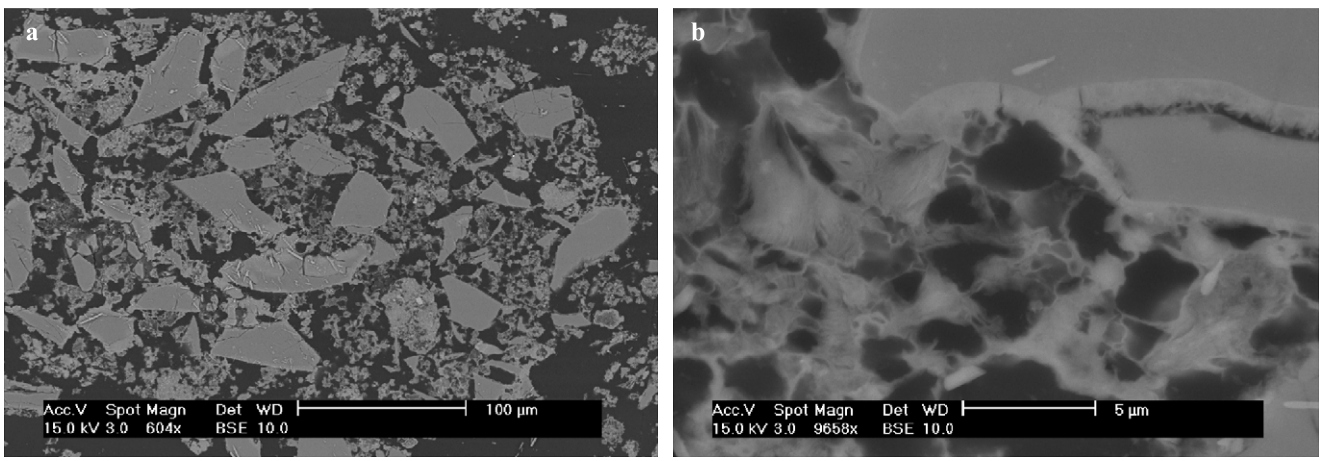

Fig. 6. BSE images of Vycor glass reacted with $Ca(OH)_2$ and KOH solution for 21 days. (a) A relatively low magnification image showing angular Vycor grains, bright coating of dense C-S-H, and C-S-H and Portlandite between grains; (b) a higher magnification image showing details of the bright C-S-H coating around the Vycor, with C-S-H and Portlandite outside the grain.

and the presence of lime increases the rate and extent of dissolution for both opal and Vycor, consistent with the results for the reaction experiments described above. The opal cubes are trapezoidal in shape after reaction, with the smaller top indicating greater dissolution there. The Vycor cubes show no change in shape or even roughening of their surfaces. The surface of the opal cubes in contact with NaOH solution only was covered with a very thin layer of soft material that cracked on drying. There is too little of the material to examine. In contrast, the opal cubes in the $NaOH + Ca(OH)_2$ mixtures were covered by a shell of hard white precipitate over their entire surface. This precipitate could be easily peeled off, and its XRD powder pattern shows weak peaks for portlandite, the basal diffraction and one peak at ~29° 2θ for C-S-H, and a broad band for amorphous material (Fig. 7). The ^{29}Si MAS NMR spectrum of the precipitate contains peaks at -79.5 and -85 ppm assigned to a relatively polymerized C-S-H, and a broad band at more negative chemical shift assigned to A-S-H (Fig. 7).

Results of the opal cube experiments are very similar to those by Dent Glasser and Kataoka [2], except that we do not see the "silica garden"-like outgrowths that formed above the silica gel pieces in their experiments. Their best developed outgrowths occurred in 0.015 M KOH solution saturated with $Ca(OH)_2$. At KOH concentrations greater than 0.1 M, the dissolution of silica was so rapid that no outgrowths formed, and instead, C-S-H formed throughout the sample [2]. In our experiments, the initial NaOH concentration was 1 M, although our opal is presumably less reactive than their silica gel. Dent Glasser and Kataoka [2] identified C-S-H based on its macroscopic appearance and composition from electron microscopy but not based on XRD. The shells formed around the opal cubes reported here consist of C-S-H, A-S-H, and a trace of $Ca(OH)_2$ as indicated by the XRD and ^{29}Si NMR data. Since our experiments used more realistic aggregates and NaOH solution concentrations, they provide stronger evidence that reactions similar to those documented by Dent Glasser and Kataoka [2] and elaborated below occur at the site of ASR in in-service concrete.

3.3. Standard mortar bars

XRD and ^{29}Si MAS NMR analysis of the ASTM C1260 15- and 28-day mortar bars made with Vycor indicate formation of polymerized C-S-H and A-S-H at both times, and decrease of reactive aggregate and nearly complete consumption of $Ca(OH)_2$ by 28 days (Fig. 8). At 15 days, XRD shows peaks near 29° and 31° 2θ representing C-S-H, sharp peaks near 18° and 34° 2θ representing Portlandite formed during hydration, and a broad shoulder centered at 22° 2θ due to Vycor glass. At 28 days, the peaks for C-S-H do not change significantly, but the relative intensity of the peak for Vycor decreases substantially and the peaks for Portlandite are barely visible. The ^{29}Si MAS NMR spectra contain resonances at -79, -85, -94, and -112 ppm, which are assigned to C-S-H (Q^1 and Q^2), A-S-H (Q^3), and residual Vycor (Q^4), respectively (Fig. 8). At 15 days, the relative intensity ratios are $Q^1{:}Q^2{:}Q^3 = 1.0{:}8.9{:}4.0$. At 28 days, the ^{29}Si MAS NMR spectrum is not qualitatively different, but the $Q^1{:}Q^2{:}Q^3$ relative intensities are 1.0:11.2:4.6, indicating a slightly more polymerized C-S-H and slightly more A-S-H gel formation (quantification of Q^4 was not done due to the long T_1 for Vycor).

Optical microscopy of the 15-day mortar sample shows a typical hydrated portland cement microstructure. The Vycor remains uniform except for cracks and occasional reaction rims that have higher optical birefringence than Vycor. Most of the A-S-H occurs in voids or in the cracks. Concentric bands (~ 10 μm thick) with radiating cracks and slightly higher relief often occur around gel grains. Many of these bands have a birefringence similar to the paste.

For the opal mortar bars, XRD of the 28-day sample shows strong calcite and dolomite peaks, expected because 95% of the aggregate was limestone, and weaker peaks for portlandite, brucite, quartz, and C-S-H (data not shown). The ^{29}Si NMR spectrum of this sample contains resonances at -79, -81.5, -85, and -92 ppm, with relative intensities of 1.0:0.5:7.7:1.2. The first three resonances are due to C-S-H and the one at -92 ppm is due to A-S-H gel (data not shown). Optical microscopy of this sample shows that residual opal grains are rare. Their edges appear to be

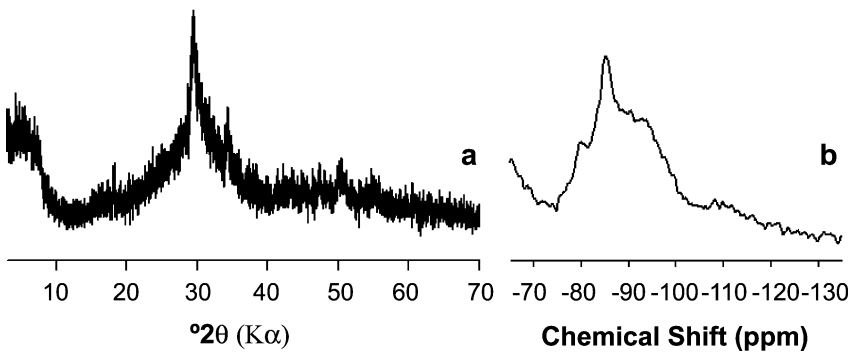

Fig. 7. (a) Powder XRD pattern and (b) ^{29}Si MAS NMR spectrum of shell precipitated on opal cubes reacted with $Ca(OH)_2$ and NaOH solution at 80° C for 1 day.

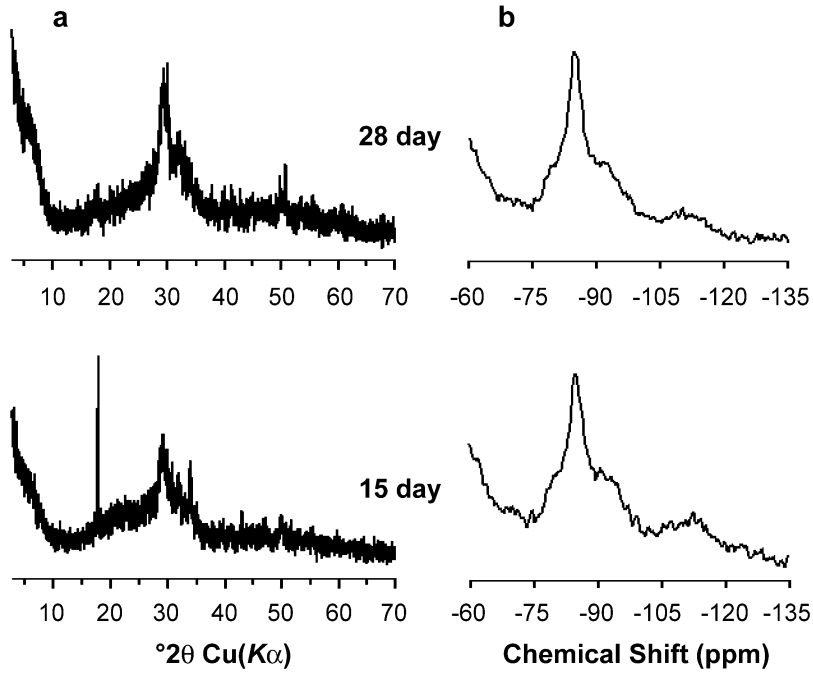

Fig. 8. (a) Powder XRD patterns and (b) ^{29}Si MAS NMR spectra of Vycor mortar bars after reaction under the conditions of ASTM C 1260 (1 M NaOH solution at 80° C) for 15 and 28 days.

dissolved and are not sharp. A-S-H occurs around such opal grains and is small in quantity.

4. Discussion

4.1. Reaction sequence

The experiments described above provide new evidence for the processes and conditions under which hydrous alkali silica gel (A-S-H) forms, its relationship to the formation of C-S-H, and the role of calcium in the reaction. The sequence of phase formation and transformation observed in the experiments described here, combined with the results of our earlier study of A-S-H formation in the laboratory and in-service concrete [26,27] and with recent advances in understanding the structure of C-S-H, its compositional relationships, and its formation in in-service concrete, support the following model for the formation and transformation of A-S-H in concrete and mortar.

The initial hydration of cement produces the normal portland cement hydration products, in particular a disordered, relatively depolymerized C-S-H [24,38,41–43,49]. After the initial hydration stage, the pore solution becomes highly alkaline, and OH^- attack on reactive aggregate causes its dissolution [1,50–52]. This silica reacts with $Ca(OH)_2$ to produce additional depolymerized C-S-H, fundamentally a pozzolanic reaction [38,53]. Once the lime is depleted within the distance over which effective chemical transport occurs, the silica released by aggregate dissolution reacts with existing C-S-H to make a more polymerized (more Si rich) C-S-H. Once the C-S-H reaches what is probably its maximum silica content (Q^1/Q^2 ratio of about 0.45 as determined from the 264-day Vycor + NaOH + $Ca(OH)_2$ reaction experiment), the silica content in the solution increases further until gelation of the A-S-H begins. With increasing time, the A-S-H transforms from a network of polymerized polyanions to a structure dominated by nanosized units with a layer structure, probably with significant cross-linking [26,27]. Once it leaves its site of origin, the A-S-H can further react with CH and C-S-H to produce a more Ca-rich and Si-poor gel [6]. There is published evidence for the absence of A-S-H during the initial stages of cement hydration [38,49,53] and the results reported here confirm this in the reaction experiments. The dissolution of silica by OH^- attack is well understood both macroscopically and on the molecular scale [1,48,51,54–58], and the increase in silica concentration in solution with increasing free energy of the solid phase is well documented [59,60]. Aggregate phases that are usually considered expansive, including opal, tridymite, cristobalite, and silica glass, have higher Gibbs free energies than the stable polymorph, quartz [1,8,9,59,60].

The observation that consumption of $Ca(OH)_2$ to form C-S-H and progressive polymerization of the C-S-H occurs before formation of A-S-H is novel here. The SEM observations showing the absence of portlandite in the vicinity of the reacting aggregate grains and the disappearance or decrease of CH as detected by XRD with reaction progress confirm the consumption of CH. The experiments of Cong et al. [23], Brough et al. [24], our previous synthesis experiments [26,27], the NMR spectra of the opal cube

samples and ASR-affected mortar bars shown in Figs. 7 and 8, and the experiments with opal + NaOH + CH (Fig. 1), show clearly that A-S-H occurs only with Q^2-dominated C-S-H. The results of the Vycor + KOH + $Ca(OH)_2$ experiments (Figs. 4 and 5) are key to demonstrating the reaction sequence and clearly show progressive polymerization of the C-S-H before formation of A-S-H.

The structural change of C-S-H from a Q^1-dominated, depolymerized form to a Q^2-dominated polymerized form requires a corresponding compositional change due to charge balance requirements [42]. Q^1 Si tetrahedra carry a net -3 charge, whereas Q^2 tetrahedra have only a net -2 charge. In alkali-free systems, this change in charge causes the Ca/Si ratio to decrease, but in alkali-rich systems the polymerized C-S-H is known to incorporate significant amounts of alkali [61–63].

Thomas [6] and Wang and Gillott [16] also suggested that Ca may exchange with alkalis in ASR gels, thereby recycling the alkalis and making them available for further ASR reaction. Thomas [6] reported composition differences between gels near or within aggregates and those far from aggregates as evidence, with large C/S ratios far from aggregates (Fig. 6 in the paper). Our current and previously published data [26,27] demonstrate that dissolved silica may react with $Ca(OH)_2$ and depolymerized C-S-H to form more polymerized C-S-H, and that A-S-H readily reacts with CH. Whether this reaction involves simple Ca for Na(K) exchange and recycling of alkalis in cement paste needs further investigation. Quantitatively, exchange of Ca for Na(K) would occur at a molar Ca/alkali ratio of 1/2, which cannot cause C/S ratios as high as reported by Thomas [6].

Based on the observation of portlandite and A-S-H in our Vycor mortar bar samples, we speculate that in concrete and mortar a reactive transport barrier around aggregate grains is needed to allow development of the high solution silicate concentrations needed to produce ASR gel. Others have previously proposed such a barrier [6,13]. The data presented here shows that such barriers probably consist of Si-rich, polymerized C-S-H. These barriers need not be continuous or completely impermeable. Rather, they simply need to provide a mechanism to prevent Si from migrating too rapidly out from the site of dissolution and Ca from migrating too rapidly in. In a recent study on the reactivity of Pyrex rods embedded in a mortar, Yi and Ostertag [64] reported distinctive banded distributions of Ca- and Na-rich gels around the Pyrex rods. The gel closer to the mortar matrix exhibits a higher Ca concentration and a lower Na concentration compared to the gel closer to the Pyrex rods. These observations support the idea of a reactive barrier and our suggested reaction sequence as well.

The data presented here are consistent with many previous observations showing that Ca^{2+} is essential to significant formation of A-S-H and ASR-related expansion. In addition to being essential for the formation of a transport barrier composed of polymerized C-S-H, Ca^{2+} significantly increases the rate of reactive silica dissolution, at least at the initial stages, by maintaining a low solution silica concentration.

4.2. K versus Na

Comparison of the XRD and ^{29}Si NMR data for the opal and Vycor samples reacted with NaOH or KOH, with $Ca(OH)_2$ or without $Ca(OH)_2$, and the previous results of Cong et al. [23] indicate that K and Na behave very similarly in the ASR except that reaction rates for the K systems appear to be faster. The change from Q^1-dominant to Q^2-dominant C-S-H occurs between 7 and 21 days in the opal + NaOH + $Ca(OH)_2$ samples, between 21 and 264 days in the Vycor + KOH + $Ca(OH)_2$ samples, and is not complete by 360 days for the Vycor + NaOH + $Ca(OH)_2$ samples (in which no A-S-H is observed), although the Q^1/Q^2 in this latter system does decrease continuously. The consistently smaller Q^1/Q^2 ratios in the Vycor + KOH + $Ca(OH)_2$ samples compared to the Vycor + NaOH + $Ca(OH)_2$ samples at similar reaction times indicate faster reaction in the samples with K. This conclusion is consistent with previous reports. Wijnen et al. [65] demonstrated that dissolution of silica in various alkali hydroxide solutions is fastest in KOH. Others have shown that in alkali silicate solutions the concentration of ion pairs involving large anions increases with increasing cation size [48,66–70], and ion pair formation promotes silicate condensation by weakening the electrostatic repulsion between anions [71].

5. Conclusions

The results presented here and in our previous papers [26,27] provide strong evidence that the A-S-H reaction products and the reaction sequence in our laboratory experiments are similar to those in mortar and concrete undergoing ASR. Based on these results, we propose that A-S-H development in mortar and concrete involves a reaction sequence of normal cement hydration (including production of CH and Ca-rich, depolymerized C-S-H), increase in the alkali concentration and pH of the pore solution, attack of OH^- on the reactive aggregate, consumption of the released silica by its reaction with CH to form C-S-H until the CH is locally consumed, followed by consumption of the released silica by reaction with depolymerized, Ca-rich C-S-H to form more polymerized, Si-rich C-S-H, and finally increase of the solution silica concentration until gelation to A-S-H gel occurs. Prior to the A-S-H formation, this reaction sequence is very similar to the pozzolanic reaction in terms of forming more polymerized C-S-H by consuming reactive silica and Ca. Both K and Na behave very similarly in the ASR reaction, but the rate of reaction appears to be faster with K than with Na. Opal is significantly more reactive than Vycor glass due to dissolution and A-S-H formation in grain interiors.

Acknowledgements

The research was supported by a DOT pooled research fund managed by the Federal Highway Administration (FHWA). We would like to thank Jun-ho Shin for providing the mortar samples.

References

[1] L.S. Dent Glasser, N. Kataoka, The chemistry of 'alkali–aggregate' reaction, Cem Concr Res 11 (1981) 1–9.
[2] L.S. Dent Glasser, N. Kataoka, On the role of calcium in the alkali–aggregate reaction, Cem Concr Res 12 (1982) 321–331.
[3] S. Diamond, Chemistry and other characteristics of ASR gels, 11th International Conference on Alkali–Aggregate Reaction, 2000, pp. 31–40.
[4] L.J. Struble, Swell and other properties of synthetic alkali silica gels, Purdue University, Centre de Recherche Interuniversitaire sur le Beton (CRIB, Laval and Sherbrooke Universities), Quebec, Canada, 1979, p. 150.
[5] T. Knudsen, N. Thaulow, Quantitative microanalyses of alkali–silica gel in concrete, Cem Concr Res 5 (1975) 443–454.
[6] M. Thomas, The role of calcium hydroxide in alkali recycling in concrete, Calcium Hydroxide in Concrete, Mater. Sci. Concr., (2001) 225–236 (special issue).
[7] R. Helmuth, D. Stark, Alkali–silica reactivity mechanisms, Mater Sci Concr 3 (1992) 131–208.
[8] T.C. Powers, H.H. Steinour, An interpretation of some published researches on the alkali–aggregate reaction. II. A hypothesis concerning safe and unsafe reactions with reactive silica in concrete, J Am Concr Inst 26 (1955) 785–810.
[9] T.C. Powers, H.H. Steinour, An interpretation of some published researches on the alkali–aggregate reaction: I. The chemical reactions and mechanism of expansion, J Am Concr Inst 26 (1955) 497–516.
[10] D. Stark, Alkali–silica reactions, in P. Klieger, J. Lamond, Significance of Tests and Properties of Concrete and Concrete-Making Materials, STP 169C, American Society for Testing and Materials, Philadelphia PA, USA, 1994, pp. 365–371.
[11] L. Struble, S. Diamond, Unstable swelling behavior of alkali silica gels, Cem Concr Res 11 (1981) 611–617.
[12] L.J. Struble, S. Diamond, Swelling properties of synthetic alkali silica gels, J Am Ceram Soc 64 (1981) 652–655.
[13] R.F. Bleszynski, M.D.A. Thomas, Microstructural studies of alkali–silica reaction in fly ash concrete immersed in alkaline solutions, Adv Cem Based Mater 7 (1998) 66–78.
[14] M.D.A. Thomas, The role of calcium in alkali–silica reaction, Materials Science of Concrete (Sidney Diamond Symposium), The American Ceramic Society, Ohio, USA, 1998, pp. 325–337, special volume.
[15] L.J. Struble, The influence of cement pore solution on alkali–silica reaction, Purdue University, 1987, p. 281.
[16] H. Wang, J.E. Gillott, Mechanism of alkali–silica reaction and the significance of calcium hydroxide, Cem Concr Res 21 (1991) 647–654.
[17] F. Gaboriaud, A. Nonat, D. Chaumont, A. Craievich, Aggregation and gel formation in basic silico–calco–alkaline solutions studied: a SAXS, SANS, and ELS study, J Phys Chem B 103 (1999) 5775–5781.
[18] P.J.M. Monteiro, K.S. Wang, G.M.C. dos Santos, W.P. de Andrade, Influence of mineral admixtures on the alkali–aggregate reaction, Cem Concr Res 27 (1997) 1899–1909.
[19] M. Prezzi, P.J.M. Monteiro, G. Sposito, The alkali–silica reaction: Part I. Use of the double-layer theory to explain the behavior of reaction-product gels, ACI Mater J 94 (1997) 10–17.
[20] M. Prezzi, P.J.M. Monteiro, G. Sposito, Alkali–silica reaction: Part 2. The effect of chemical admixtures, ACI Mater J 95 (1998) 3–10.
[21] S.J. Way, A. Shayan, Synthesis and characterization of crystalline analogues of alkali–aggregate reaction products, Cem Concr Res 23 (1993) 471–479.
[22] W.F. Cole, C.J. Lancucki, Products formed in an aged concrete. The occurrence of okenite, Cem Concr Res 13 (1983) 611–618.
[23] X.D. Cong, R.J. Kirkpatrick, S. Diamond, Silicon-29 MAS NMR spectroscopic investigation of alkali silica reaction product gels, Cem Concr Res 23 (1993) 811–823.
[24] A.R. Brough, C.M. Dobson, I.G. Richardson, G.W. Groves, Alkali activation of reactive silicas in cements: in situ ^{29}Si MAS NMR studies of the kinetics of silicate polymerization, J Mater Sci 31 (1996) 3365–3373.
[25] K.E. Kurtis, P.J.M. Monteiro, J.T. Brown, W. Meyer-Ilse, Imaging of ASR gel by alkali silicate gels, Cem Concr Res 28 (1998) 411–421.
[26] X. Hou, L.J. Struble, P.J.M. Monteiro, R.J. Kirkpatrick, Structural investigations of alkali silicate gels, J. Am. Ceram. Soc. in press.
[27] X. Hou, R.J. Kirkpatrick, L.J. Struble, J.-h. Shin, P.J.M. Montiero, The structure of ASR gel and its relationship to C-S-H, in: D. Lange, K. L. Scrivener, J. Marchand (Eds.), Engineering Conference on Advances in Cement and Concrete IX: Volume Changes, Cracking, and Durability, Copper Mountain, Colorado, (2003) 365–376. University of Illinois at Urbana-Champaign.
[28] K.E. Kurtis, P.J.M. Monteiro, J.T. Brown, W. Meyer-Ilse, Investigation of alkali–silica reaction by transmission soft X-ray microscopy, AIP Conf Proc 507 (2000) 213–218 (X-ray Microscopy).
[29] W. Wieker, C. Hubert, D. Deidemann, Recent results of solid-state NMR investigations and their possibilities of use in cement chemistry, Proceedings International Congress Chemistry of Cement, 10th, vol. 1, Amarkai AB, Sweeden, 1997, pp. 2–24.
[30] W. Wieker, C. Hubert, D. Heidemann, R. Ebert, Alkali–silica reaction—a problem of the insufficient fundamental knowledge of its chemical base, Materials Science of Concrete (Sidney Diamond Symposium), The American Ceramic Society, Ohio, USA, 1998, pp. 395–408 (special volume).
[31] W. Wieker, C. Hubert, D. Heidemann, R. Ebert, Some experiences in chemical modelling of the alkali–silica reaction, 11th International Conference on Alkali–Aggregate Reaction, 2000. Centre de Recherche Interuniversitaire sur le Beton (CRIB, Laval and Sherbrooke Universities), Quebec, Canada. 119–128.
[32] W. Wieker, D. Heidemann, R. Ebert, A. Tapper, Chemistry of kanemite $[NaHSi_2O_3 \times 3H_2O]x$, Z Anorg Allg Chem 621 (1995) 1779–1784.
[33] L.A.J. Garvie, B. Devouard, T.L. Groy, F. Camara, P.R. Buseck, Crystal structure of kanemite, $NaHSi_2O_5 \times 3H_2O$, from the Aris phonolite, Namibia, Am Miner 84 (1999) 1170–1175.
[34] S. Vortmann, J. Rius, B. Marler, H. Gies, Structure solution from powder data of the hydrous layer silicate kanemite, a precursor of the industrial ion exchanger SKS-6, Eur J Mineral 11 (1999) 125–134.
[35] S.A. Marfil, P.J. Maiza, Zeolite crystallization in portland cement concrete due to alkali–aggregate reaction, Cem Concr Res 23 (1993) 1283–1288.
[36] S.A. Marfil, P.J. Maiza, Deteriorated pavements due to the alkali–silica reaction. A petrographic study of three cases in Argentina, Cem Concr Res 31 (2001) 1017–1021.
[37] W. Prince, G. Castanier, J.L. Giafferi, Similarity between alkali–aggregate reaction and the natural alteration of rocks, Cem Concr Res 31 (2001) 271–276.
[38] H.F.W. Taylor, Cement Chemistry, 2nd ed., Thomas Telford Publishing, Thomas Telford Services, London, 1997, p. 459.
[39] The American Society for Testing Materials (ASTM), Standard method for potential alkali–silica reactivity of aggregates (mortar bar method), Concrete and Aggregates, C-1260-94, Annual Book of ASTM Standards, vol. 04.02, ASTM, Philadelphia, 1994, pp. 648–651.
[40] H. Graetsch, H. Gies, I. Topalovic, NMR, XRD and IR study on microcrystalline opals, Phys Chem Miner 21 (1994) 166–175.
[41] X. Cong, Silicon-29 and Oxygen-17 Nuclear Magnetic Resonance Investigation of the Structure of Calcium–Silicate–Hydrate (Ce-

ment), University of Illinois at Urbana-Champaign, Urbana, IL, 1994, p. 171.
[42] X. Cong, R.J. Kirkpatrick, ^{29}Si MAS NMR study of the structure of calcium silicate hydrate, Adv Cem Based Mater 3 (1996) 144–156.
[43] X. Cong, R.J. Kirkpatrick, ^{29}Si and ^{17}O NMR investigation of the structure of some crystalline calcium silicate hydrates, Adv Cem Based Mater 3 (1996) 133–143.
[44] F. Gaboriaud, A. Nonat, D. Chaumont, A. Craievich, B. Hanquet, ^{29}Si NMR and small-angle X-ray scattering studies of the effect of alkaline ions (Li^+, Na^+, and K^+) in silico-alkaline sols, J Phys Chem B 103 (1999) 2091–2099.
[45] W. Wieker, Structure of silicates in solution and in the solid state, Kem Kozl 65 (1986) 233–249.
[46] R.K. Harris, E.K.F. Bahlmann, K. Metcalfe, E.G. Smith, Quantitative silicon-29 NMR investigations of highly concentrated high-ratio sodium silicate solutions, Magn Reson Chem 31 (1993) 743–747.
[47] S.D. Kinrade, T.W. Swaddle, Silicon-29 NMR studies of aqueous silicate solutions: 1. Chemical shifts and equilibria, Inorg Chem 27 (1988) 4253–4259.
[48] P.W.J.G. Wijnen, T.P.M. Beelen, J.W. De Haan, C.P.J. Rummens, L.J.M. Van de Ven, R.A. Van Santen, Silica gel dissolution in aqueous alkali metal hydroxides studied by silicon-29 NMR, J Non-Cryst Solids 109 (1989) 85–94.
[49] J.F. Young, Investigation of calcium silicate hydrate structure using silicon-29 nuclear magnetic resonance spectroscopy, J Am Ceram Soc 71 (1988) C118–C120.
[50] S. Diamond, Alkali silica reactions—some paradoxes, Cem Concr Compos 19 (1997) 391–401.
[51] K.E. Kurtis, C.L. Collins, P.J.M. Monteiro, The surface chemistry of the alkali–silica reaction: a critical evaluation and X-ray microscopy, Concr Sci Eng 4 (2002) 2–11.
[52] F.P. Glasser, Chemistry of the alkali–aggregate reaction, in: R.N. Swamy (Ed.), The Alkali Silica Reaction in Concrete, Blackie, Glasgow, UK, 1992, pp. 30–53.
[53] M.S.Y. Bhatty, Mechanism of pozzolanic reactions and control of alkali–aggregate expansion, Cem., Concr Aggreg 7 (1985) 69–77.
[54] D. Bulteel, E. Garcia-Diaz, C. Vernet, H. Zanni, Alkali–silica reaction. A method to quantify the reaction degree, Cem Concr Res 32 (2002) 1199–1206.
[55] L. Fernandez, H. Zanni, R. Couty, P. Barret, D. Bertrandie, Contribution of silicon-29 high-resolution NMR to the study of concrete alkali–aggregates reaction, J Chim Phys 89 (1992) 453–460.
[56] W.H. Casey, A.C. Lasaga, G.V. Gibbs, Mechanisms of silica dissolution as inferred from the kinetic isotope effect, Geochim Cosmochim Acta 54 (1990) 3369–3378.
[57] M.A.T.M. Broekmans, J.B.H. Jansen, Silica dissolution in impure sandstone: application to concrete, J Geochem Explor 62 (1988) 311–318.
[58] S.A. Carroll, R.S. Maxwell, W. Bourcier, S. Martin, S. Hulsey, Evaluation of silica–water surface chemistry using NMR spectroscopy, Geochim Cosmochim Acta 66 (2002) 913–926.
[59] S. Diamond, A review of the alkali–silica reaction and expansion mechanisms: 2. Reactive aggregates, Cem Concr Res 6 (1976) 549–560.
[60] A.B. Poole, Alkali silica reactivity mechanisms of gel formation and expansion, International Conference on Alkali–Aggregate Reaction in Concrete, 9th, vol. 2, Concr. Soc., UK, 1992, pp. 782–789.
[61] H. Viallis, P. Faucon, J.-C. Petit, A. Nonat, Interaction between salts (NaCl, CsCl) and calcium silicate hydrates (C-S-H), J. Phys. Chem. B. 1999, 103 5212–5219.
[62] N. Hara, N. Inoue, H. Noma, Thermal behaviour of tobermorite intercalated with alkali cations, 10th International Congress on the Chemistry of Cement, Gothenburg, Sweden, vol. 2, 1997, Amarkai AB, Sweden, 2ii065–5 pp.
[63] I. Lognot, I. Klur, A. Nonat, NMR and infrared spectroscopies of C-S-H and Al substituted C-S-H synthesized in alkaline solution, in: P. Colombet, A.R. Grimmer, H. Zanni, P. Sozzani (Eds.), Nuclear Magnetic Resonance Spectroscopy of Cement Based Material, Springer-Verlag, Berlin, 1998, pp. 189–196.
[64] C. Yi, C.P. Ostertag, Effect of steel microfibers on alkali silica reaction, Engineering Conference International (ECI): Advances in Cement and Concrete IX, Copper Mountain, Colorado, USA. University of Illinois at Urbana–Champaign, 2003, pp. 249–255.
[65] P.W.J.G. Wijnen, T.P.M. Beelen, J.W. De Haan, L.J.M. Van de Ven, R.A. Van Santen, The structure directing effect of cations in aqueous silicate solutions—A silicon 29 NMR stade, Colloids Surf 45 (1990) 255–268.
[66] J. Sanchez, A. McCormick, NMR and theoretical investigation of cation binding with sol–gel silicates, Chem Mater 3 (1991) 320–324.
[67] A.V. McCormick, A.T. Bell, C.J. Radke, The influence of alkali metal hydroxides on silica condensation rates: the role of ion pairing, Mater Res Soc Symp Proc 121 (1988) 67–72 (Better Ceram. Chem. 3).
[68] P. Nieto, H. Zanni, Polymerization of alkaline–calcium–silicate hydrates obtained by interaction between alkali–silica solutions and calcium compounds. A ^{29}Si nuclear magnetic resonance study, J Mater Sci 32 (1997) 3419–3425.
[69] H. Zanni, P. Nieto, L. Fernandez, R. Couty, P. Barret, A. Nonat, D. Bertrandie, Sol–gel transition in silica alkaline solutions. A NMR study, J Chim Phys 91 (1994) 901–908.
[70] A.V. McCormick, A.T. Bell, C.J. Radke, Evidence from alkali–metal NMR spectroscopy for ion pairing in alkaline silicate solutions, J Phys Chem B 93 (1989) 1733–1737.
[71] S.D. Kinrade, D.L. Pole, Effect of alkali–metal cations on the chemistry of aqueous silicate solutions, Inorg Chem 31 (1992) 4558–4563.